Journal Name

RSCPublishing

ARTICLE

Ammonia Borane - Metal Alanate composites: hydrogen desorption properties and decomposition processes

Cite this: DOI: 10.1039/xoxxoooooox

Received ooth January 2012,
Accepted ooth January 2012

DOI: 10.1039/xoxxoooooox

www.rsc.org/

Yuki Nakagawa,[*a] Yudai Ikarashi,[a] Shigehito Isobe,[*ab] Satoshi Hino[a] and Somei Ohnuki[a]

Hydrogen desorption properties and decomposition processes of NH_3BH_3-$MAlH_4$ (M = Na, Li) composites were investigated by using thermogravimetry-differential thermal analysis (TG-DTA-MS), powder X-ray diffraction (XRD) and Fourier transform infrared spectroscopy (FTIR) analyses. We prepared the composites by ball-milling and the mixtures by hand-milling. The ball-milled composites desorbed 4-5 wt% hydrogen at three exothermic steps below 260 °C. The emissions of by-product gases, NH_3, B_2H_6 and $B_3H_6N_3$, were effectively suppressed. From XRD and FTIR analyses, the formation of mixed-metal (Na(Li), Al) amidoborane phase was suggested. Very different results were obtained using hand-milling. They showed only one exothermic reaction at 80-90 °C. The emission of by-product gases was not suppressed. By comparing the differences between ball-milled composites and hand-milled mixtures, the importance of mixed-metal amidoborane in this system was proposed.

1. Introduction

Ammonia borane (NH_3BH_3, AB) is considered as one of the most promising hydrogen storage materials because of its high hydrogen capacity (19.6 wt%, 0.145 kg L^{-1}) and relatively low dehydrogenation temperature.[1] Nevertheless, sluggish kinetics below 100 °C, poor recyclability, and emission of by-product gases during heating (e.g., ammonia (NH_3), diborane (B_2H_6) and borazine ($B_3H_6N_3$)) are disadvantages for practical applications.[2-4] For instance, release of ammonia causes damage to the fuel cell performance even at trace levels.[5] Also, NH_3 and B_2H_6 are toxic materials for living things.[6, 7]

To overcome these disadvantages, several approaches have been developed, such as infusion of AB in nanoscaffolds,[8] doping with transition metals as catalysts,[9] size and catalytic effects from graphitic carbon nitride,[10] and chemical modification of AB by replacing one of H atoms with an alkali or alkaline earth metal to form metal amidoboranes.[11] In previous reports, many kinds of AB-MH (Metal Hydride) composites, such as AB-LiH,[11-16] AB-NaH,[11-13,17,18] AB-KH,[12,13,19] AB-MgH_2,[20,21] AB-CaH_2,[20] AB-$LiNH_2$,[22] AB-$LiBH_4$,[23] and AB-Li_3AlH_6,[24] were synthesized and their dehydrogenation properties were investigated. Recently, we experimentally verified that AB-$MAlH_4$ (M = Na, Li) composites, which were prepared based on the indicator we proposed, can suppress the emission of NH_3, B_2H_6 and $B_3H_6N_3$.[25] However, their decomposition processes have not been clarified yet.

In this study, we investigated the decomposition processes of AB-$MAlH_4$ (M = Na, Li) composites. We prepared the composites by ball-milling and the mixtures by hand-milling. We analysed the hydrogen desorption properties by thermogravimetry-differential thermal analysis-mass spectrometry (TG-DTA-MS) and performed phase identification by powder X-ray diffraction (XRD) and Fourier transform infrared (FTIR) spectroscopy. By comparing the ball-milled composites and hand-milled mixtures, the decomposition processes were proposed.

2. Experimental

The starting materials NH_3BH_3, $NaAlH_4$, $LiAlH_4$ (purity 97 %, 90 %, 95 %, respectively) were purchased from Sigma Aldrich Co. Ltd. These materials were used as-received without any purification. All samples were handled in an argon-filled glovebox to prevent sample oxidation. AB-$MAlH_4$ (M = Na, Li) composites were prepared by ball-milling of AB and $MAlH_4$ (M = Na, Li) with a molar ratio of 1 : 1 under a 1.0 MPa H_2 atmosphere with 300 rpm for 5 min. Ball-milling was performed by using a planetary ball-mill apparatus (Fritsch Pulverisette 7) with 20 stainless steel balls (7 mm in diameter) and 300 mg samples (ball : powder ratio = 70 : 1, by mass). We also prepared the mixtures by hand-milling. Hand-milled mixtures were prepared by mixing AB and $MAlH_4$ (M = Na, Li) in an agate mortar in the glove box for 90 seconds. Hand-milling over 120 seconds is dangerous because it often causes gas eruptions. The hydrogen desorption properties were examined by thermal desorption mass spectrometry measurements (TDMS, ULVAC, BGM-102) combined with thermogravimetry and differential thermal analysis (TG-DTA, Bruker, 2000SA). The heating rate was 5 °C min^{-1} and the helium gas flow rate was 300 mL min^{-1}. Powder X-ray diffraction (XRD, PANalytical, X'Pert Pro with Cu Kα radiation) measurements were performed to observe the phases of composites. The samples used for XRD measurements were

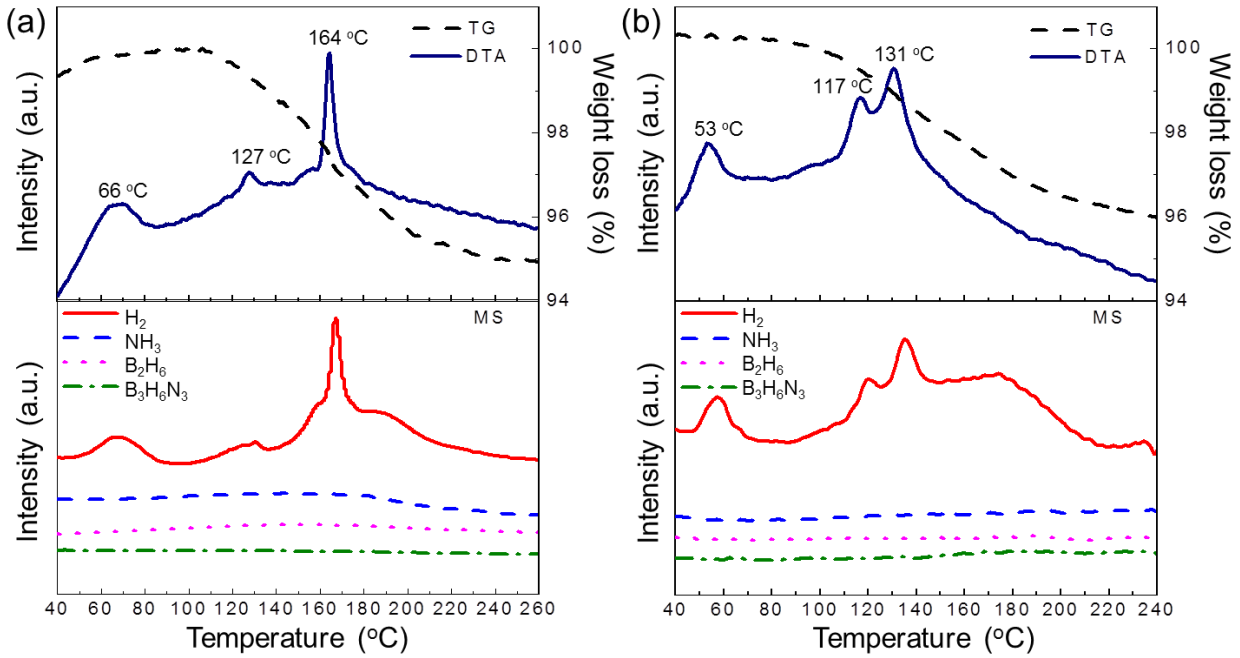

Fig. 1 TG-DTA-MS profiles of ball-milled AB-$MAlH_4$ composites; (a) AB-$NaAlH_4$ composite, (b) AB-$LiAlH_4$ composite. The heating rate was 5 °C min^{-1}.

placed on a greased glass plate in an argon-filled glovebox and then sealed with a polyimide sheet (Kapton, The Nilaco Co. Ltd.) to avoid oxidation during measurement. Fourier transform infrared spectrometry (FT-IR, Spectrum One, Perkin-Elmer) measurements were performed using a diffuse reflection cell to investigate chemical bonds in the composites. All the samples were diluted with KBr to a mass ratio of 5 : 95 (sample : KBr).

3. Results and Discussion

3.1 Hydrogen desorption properties of ball-milled composites

TG-DTA-MS results of ball-milled AB–$MAlH_4$ (M = Na, Li) composites are shown in Fig. 1. As shown in Fig. 1 (a), exothermic peaks were observed at 66, 127, and 164 °C in DTA profile of AB-$NaAlH_4$ composite. These peaks correspond to H_2 desorption peaks in mass spectra. The composite did not desorb NH_3, B_2H_6, and $B_3H_6N_3$ at all within the accuracy of our apparatus. From TG profile, the amount of desorbed H_2 was estimated at 5 wt%. AB-$LiAlH_4$ composite showed similar H_2 desorption properties as those of AB-$NaAlH_4$ composite. Three exothermic peaks (53, 117 and 131 °C) were observed in DTA profile. The composite did not desorb NH_3, B_2H_6 and $B_3H_6N_3$. The suppression of by-product gas emission was also found in AB-Li_3AlH_6 composite.[24] The amount of desorbed H_2 was about 4 wt% for AB-$LiAlH_4$ composite. These results were quite different from the TG-DTA-MS results of AB[2] or $MAlH_4$[26] (M = Na, Li) itself, suggesting the reactions between AB and $MAlH_4$ during milling and heating. Each exothermic peak of AB-$LiAlH_4$ composite was lower than the corresponding peak of AB-$NaAlH_4$ composite. This would be correlated with the lower thermal stability of $LiAlH_4$ than that of $NaAlH_4$.[27]

3.2 Structure and phase analyses of ball-milled composites

The pressure increase due to H_2 desorption was observed during ball-milling, which suggested the mixed-metal amidoborane formed by the reaction between $NaAlH_4$ and AB. NH_3, B_2H_6, and $B_3H_6N_3$ desorption was not observed during ball-milling. One of the driving forces for the reaction would be the affinity of $H^{\delta-}$ in $NaAlH_4$ and $H^{\delta+}$ in NH_3 of AB. Fig. 2 shows the XRD profiles of ball-milled AB-$MAlH_4$ (M = Na, Li) composites after heating to each temperature. Broad diffraction peaks at around 20° and 27° in all profiles originate from the polyimide film and grease to prevent sample oxidation. In AB-$NaAlH_4$ composite, both AB and $NaAlH_4$ phases were observed at room temperature (RT). Besides, small unknown peaks appeared in the range of 15 – 30°. These peaks doesn't match with any diffraction pattern of decomposition products of starting materials or mono-metal amidoborane, suggesting the formation of mixed-metal (Na, Al) amidoborane phase during ball-milling. After heating to 80 °C, the peak intensities of mixed-metal amidoborane became stronger compared to RT. The reaction between AB and $NaAlH_4$ proceeded further to form the mixed-metal amidoborane, resulting in the H_2 desorption at 66 °C as shown in Fig. 1 (a). After heating to 140 °C, the mixed-metal amidoborane phase disappeared, indicating its decomposition. It is interesting that $NaBH_4$ phase appeared at 140 °C. After heating to 170 °C, strong peak intensities of $NaBH_4$ were observed, while most of $NaAlH_4$ phase disappeared. The formation process of $NaBH_4$ will be described in Section 3.3. Furthermore, a new set of peaks were observed in the range of 10 – 25°. This could be another mixed-metal amidoborane formed by the reaction between Na_3AlH_6 and AB. After heating to 260 °C, this unknown phase decomposed and only $NaBH_4$ and Al phases were observed. In case of AB-$LiAlH_4$ composite, similar results were obtained as AB-$NaAlH_4$ composite. At RT, unknown peaks, which were considered as mixed-metal (Li, Al) amidoborane, were

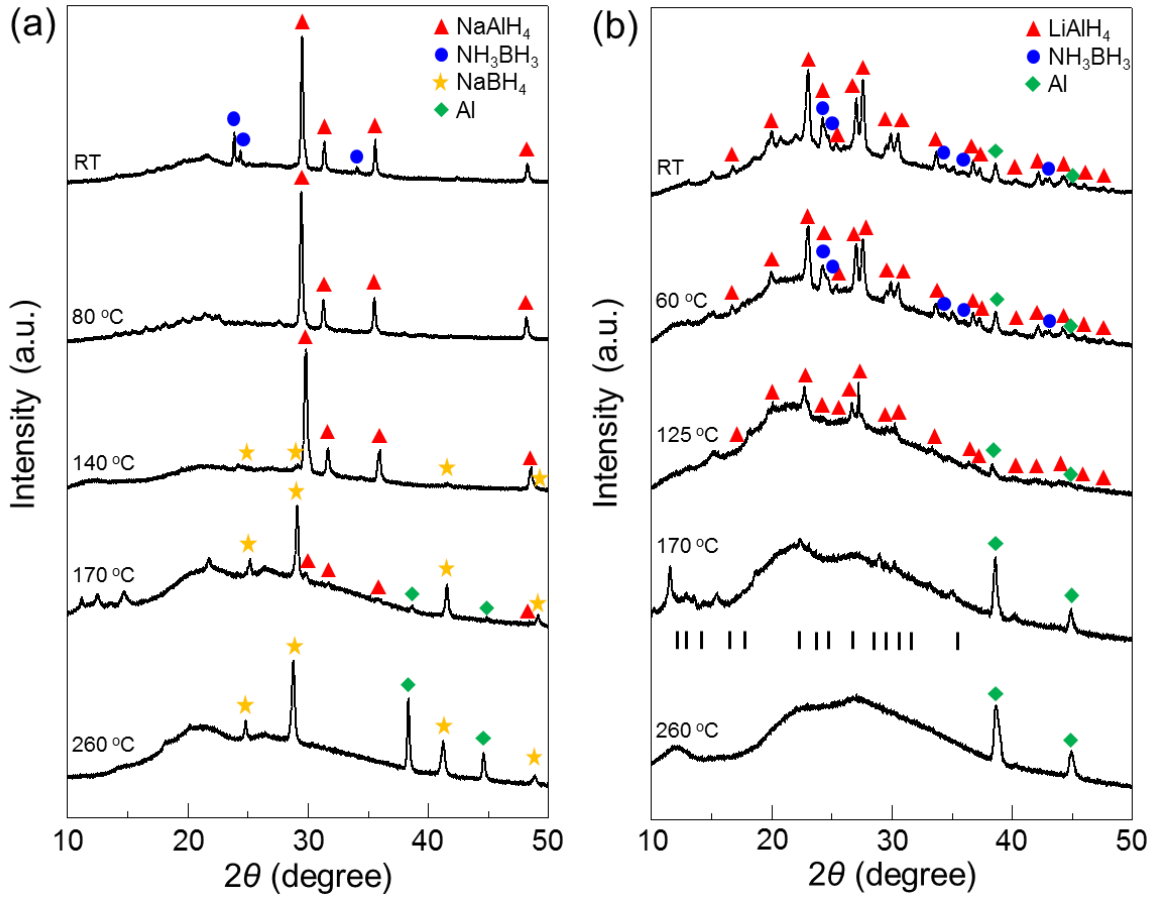

Fig. 2 XRD profiles of ball-milled AB-$MAlH_4$ composites after heating to each temperature; (a) AB-$NaAlH_4$ composite, (b) AB-$LiAlH_4$ composite.

observed in the range of 10 – 25°. After heating to 170 °C, further new peaks were observed in the range of 10 – 40°. The peak positions of AB-Li_3AlH_6 composite reported by Xia *et al.* were also shown as reference in Fig. 2 (b).[24] The positions of observed peaks were similar to the reference, suggesting the formation of mixed-metal (Li, Al) amidoborane. Though borohydride phase was not observed in the XRD profiles of AB-$LiAlH_4$ composite, the FTIR spectra showed the strong B-H stretching. This indicated that the amorphous $LiBH_4$ formed during heating.

Fig. 3 shows the *in-situ* FTIR spectra of ball-milled AB-$MAlH_4$ (M = Na, Li) composites during heating. The spectra of AB and $MAlH_4$ (M = Na, Li) at RT were also shown as references. In AB-$MAlH_4$ (M = Na, Li) composites, peak intensities corresponding to N-H stretching between 3150 and 3500 cm^{-1} decreased as temperature increased, whereas peaks corresponding to B-H stretching between 2200 and 2400 cm^{-1} were remained after heating to 260 °C in both composites. This phenomenon was also observed in other metal amidoboranes.[17,20,21,23,24] From this result, the formation of metal amidoborane phase was also suggested.

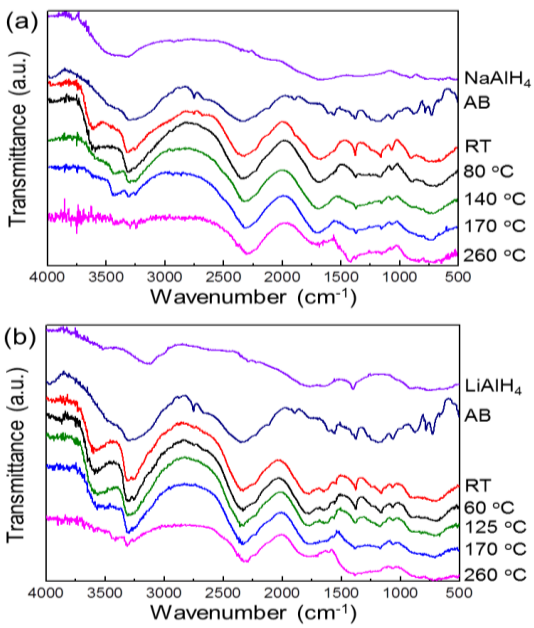

Fig. 3 *In-situ* FTIR spectra of ball-milled AB-$MAlH_4$ composites at each temperature; (a) AB-$NaAlH_4$ composite, (b) AB-$LiAlH_4$ composite. AB and $MAlH_4$ (M = Na, Li) spectra was presented for comparison. The heating rate was 5 °C min^{-1}.

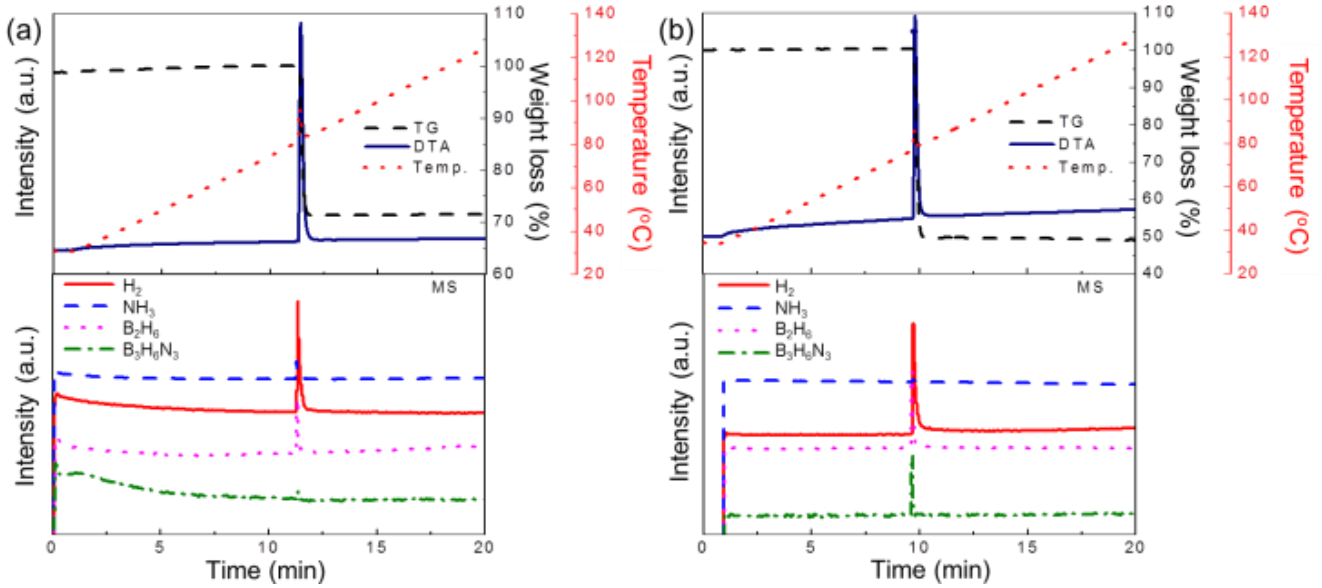

Fig. 4 TG-DTA-MS profiles of hand-milled AB-$MAlH_4$ mixtures; (a) AB-$NaAlH_4$ mixture, (b) AB-$LiAlH_4$ mixture. The heating rate was 5 °C min^{-1}.

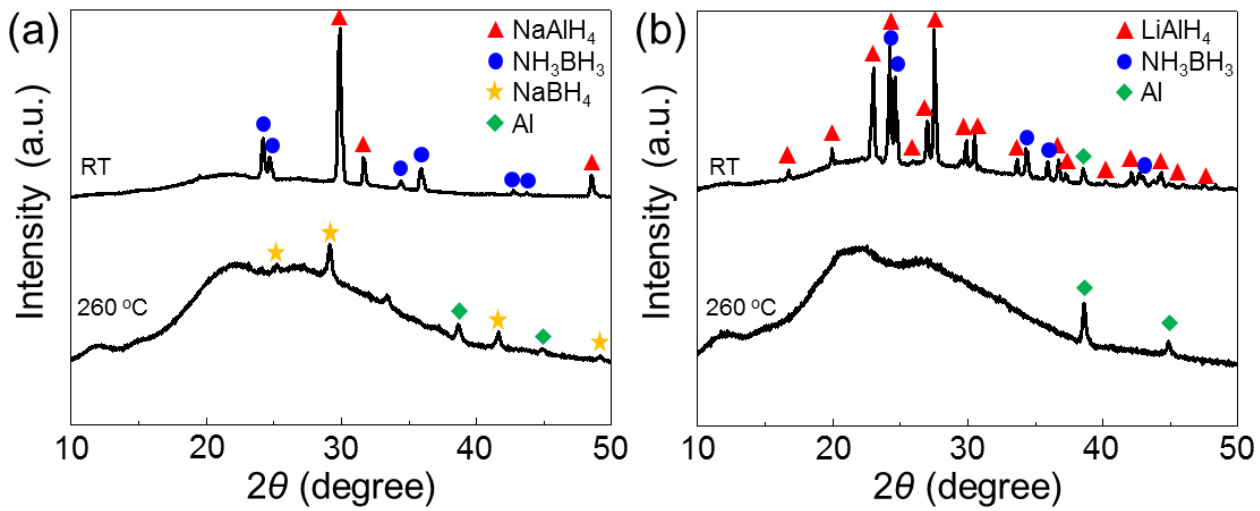

Fig. 5 XRD profiles of hand-milled AB-$MAlH_4$ mixtures at RT and after heating to 260 °C; (a) AB-$NaAlH_4$ mixture, (b) AB-$LiAlH_4$ mixture.

3.3 Comparison with hand-milled mixtures

To clarify the reaction process in detail, we prepared the mixtures by hand-milling and investigated their H_2 desorption properties and phases. Interestingly, results were quite different from the ball-milled composites. Fig. 4 shows TG-DTA-MS results of hand-milled AB–$MAlH_4$ (M = Na, Li) mixtures. Sharp exothermic peaks were observed at 90 °C (AB-$NaAlH_4$) and 84 °C (AB-$LiAlH_4$) in DTA profiles. The weight losses of about 30 wt% (AB-$NaAlH_4$) and 50 wt% (AB-$LiAlH_4$) were also observed. From the mass spectra, H_2, NH_3, B_2H_6 and $B_3H_6N_3$ peaks were observed in both mixtures. Except this exothermic reaction, any reactions were not observed up to 260 °C.

Fig. 5 shows the XRD profiles of hand-milled AB-$MAlH_4$ (M = Na, Li) mixtures before and after heating to 260 °C. Before heating, AB and $MAlH_4$ (M = Na, Li) were observed. Unknown peaks were not observed in the range of 10 – 30°, which was different from the results of ball-milled composites. After heat treatment, $NaBH_4$ was observed in the AB-$NaAlH_4$ mixture, which was similar to the results of ball-milled composites.

The reaction observed in the hand-milled mixture was quite similar to the solid state reaction of $MAlH_4$ (M = Na, Li) with NH_4Cl. In this reaction, MCl and $[H_4Al{\cdot}NH_4]$ is formed and soon $[H_4Al{\cdot}NH_4]$ decomposes to [HAlNH] and H_2, accompanied by a large exothermic heat.[28] The previous study showed diammoniate of diborane (DADB), $[(NH_3)_2BH_2]^+[BH_4]^-$, an ionic isomer of AB, is formed during the induction period before H_2 desorption occurs.[29] $MAlH_4$ was also confirmed to be an ionic compound, consisting of M^+ cation and AlH_4^- anion.[30] Considering the reaction between DADB and $NaAlH_4$, the reaction between BH_4^- anion and Na^+ cation would cause the formation of $NaBH_4$. On the one hand, the reaction between $[(NH_3)_2BH_2]^+$ and AlH_4^- would cause the H_2 and by-product gas emissions. However, the ball-milled

composites showed the different results from the hand-milled mixtures. This would be attributed to the formation of mixed-metal amidoborane. Though this phase was not observed in the hand-milled mixtures, it was observed in the ball-milled composites at not only RT but also other temperatures (e.g., 170 °C). The interaction between metal amidoborane and AB like $LiNH_2BH_3{\cdot}NH_3BH_3$ showed the significantly low H_2 desorption temperature.[15,16] Similarly, the interaction between mixed-metal amidoborane and AB could occur in the ball-milled composites. Mixed-metal amidoborane would stabilize the reaction between Al-H bonds and N-H bonds, resulting in the suppression of by-product gases. Thus, it is suggested that mixed-metal amidoborane plays an important role in suppressing the emission of by-product gases.

4. Conclusions

$AB\text{-}MAlH_4$ (M = Na, Li) composites were successfully synthesized by ball-milling and their hydrogen desorption properties and decomposition processes were investigated. The composites desorbed 4-5 wt% hydrogen below 260 °C, accompanied by H_2 desorption. They did not desorb NH_3, B_2H_6, and $B_3H_6N_3$ at all. They showed three exothermic reactions below 260 °C, accompanied by H_2 desorption. The first reaction is ascribed to the formation of mixed-metal amidoborane phase. The second reaction is ascribed to the decomposition of mixed-metal amidoborane. In the last, the reactions described as below occurred. One is the reaction between AB and $MAlH_4$ (M = Na, Li), which result in the formation of MBH_4 (M = Na, Li). The other is the reaction between M_3AlH_6 (M = Na, Li) and AB, which result in the formation of another mixed-metal amidoborane. The hand-milled mixtures showed quite different results from the ball-milled composites. They showed only one exothermic reaction at 80-90 °C. The emission of by-product gases was not suppressed. By comparing the results of the ball-milled composites with those of the hand-milled mixtures, the importance of the mixed-metal amidoborane as a barrier against by-product gas emission in this system was proposed. These results would be helpful for clarifying reaction mechanisms of AB-MH composites.

Notes and References

[a] Graduate School of Engineering, Hokkaido University, N-13, W-8, Sapporo 060-8278, Japan. E-mail: isobe@eng.hokudai.ac.jp (S. Isobe), y-nakagawa@eng.hokudai.ac.jp (Y. Nakagawa); Tel: +81-11-706-6771; FAX: +81-11-706-6772

[b] Creative Research Institution, Hokkaido University, N-21, W-10, Sapporo 001-0021, Japan

1 F. H. Stephens, V. Pons and R. T. Baker, *Dalton Trans.*, 2007, **25,** 2613-2626.
2 G. Wolf, J. Baumann, F. Baitalow and F. P. Hoffmann, *Thermochim. Acta*, 2000, **343,** 19-25.
3 F. Baitalow, J. Baumann, G. Wolf, K. J. Röβler and G. Leitner, *Thermochim. Acta*, 2002, **391,** 159-168.
4 J. Baumann, F. Baitalow and G. Wolf, *Thermochim. Acta*, 2005, **430,** 9-14.
5 N. Rajalakshmi, T. T. Jayanth and K. S. Dhathathreyan, *Fuel Cells*, 2004, **3,** 177-180.
6 International Chemical Safety Cards, ICSC number: 0414.
7 International Chemical Safety Cards, ICSC number: 0432.
8 A. Gutowska, L. Li, Y. Shin, C. M. Wang, X. S. Li, J. C. Linehan, R. S. Smith, B. D. Kay, B. Schmid, W. Shaw, M. Gutowski and T. Autrey, *Angew. Chem. Int. Ed.*, 2005, **44,** 3578-3582.
9 B. L. Conley, D. Guess and T. J. Williams, *J. Am. Chem. Soc.*, 2011, **133,** 14212-14215.
10 Z. Tang, X. Chen, H. Chen, L. Wu and X. Yu, *Angew. Chem. Int. Ed.*, 2013, **52,** 5832-5835.
11 Z. Xiong, C. K. Yong, G. Wu, P. Chen, W. Shaw, A. Karkamkar, T. Autrey, M. O. Jones, S. R. Johnson, P. P. Edwards and W. I. F. David, *Nat. Mater.*, 2008, **7,** 138-141.
12 A. T. Luedtke and T. Autrey, *Inorg. Chem.*, 2010, **49,** 3905-3910.
13 Y. Zhang and C. Wolverton, *J. Phys. Chem. C*, 2012, **116,** 14662-14664.
14 K. Shimoda, K. Doi, T. Nakagawa, Y. Zhang, H. Miyaoka, T. Ichikawa, M. Tansho, T. Shimizu, A.K. Burrell and Y. Kojima, *J. Phys. Chem. C*, 2012, **116,** 5957-5964.
15 C. Wu, G. Wu, Z. Xiong, W. I. F. David, K. R. Ryan, M. O. Jones, P. P. Edwards, H. Chu and P. Chen, *Inorg. Chem.*, 2010, **49,** 4319-4323.
16 C. Wu, G. Wu, Z. Xiong, X. Han, H. Chu, T. He and P. Chen, *Chem. Mater.*, 2010, **22,** 3-5.
17 K. J. Fijałkowski and W. Grochala, *J. Mater. Chem.*, 2009, **19,** 2043-2050.
18 K. Shimoda, Y. Zhang, T. Ichikawa, H. Miyaoka and Y. Kojima, *J. Mater. Chem.*, 2011, **21,** 2609-2615.
19 H. V. K. Diyabalanage, T. Nakagawa, R. P. Shrestha, T. A. Semelsberger, B. L. Davis, B. L. Scott, A. K. Burrell, W. I. F. David, K. R. Ryan, M. O. Jones and P. P. Edwards, *J. Am. Chem. Soc.*, 2010, **132,** 11836-11837.
20 Y. Zhang, K. Shimoda, H. Miyaoka, T. Ichikawa and Y. Kojima, *Int. J. Hydrogen Energy*, 2010, **35,** 12405-12409.
21 X. Kang, L. Ma, Z. Fang, L. Gao, J. Luo, S. Wang and P. Wang, *Phys. Chem. Chem. Phys.*, 2009, **11,** 2507-2513.
22 K. R. Graham, T. Kemmitt and M. E. Bowden, *Energy Environ. Sci.*, 2009, **2,** 706-710.
23 J. Luo, H. Wu, W. Zhou, X. Kang, Z. Fang and P. Wang, *Int. J. Hydrogen Energy*, 2012, **37,** 10750-10757.
24 G. Xia, Y. Tan, X. Chen, Z. Guo, H. Liu, and X. Yu, *J. Mater. Chem. A*, 2013, **1,** 1810-1820.
25 Y. Nakagawa, S. Isobe, Y. Ikarashi and S. Ohnuki, *J. Mater. Chem. A*, 2014, **2,** 3926-3931.
26 T. Zhang, S. Isobe, Y. Wang, H. Oka, N. Hashimoto and S. Ohnuki, *J. Mater. Chem. A*, 2014, **2,** 4361-4365.
27 T. Matsunaga, F. Buchter, K. Miwa, S. Towata, S. Orimo and A. Züttel, *Renewable Energy*, 2008, **33,** 193-196.
28 H. Zhang, Y. S. Loo, H. Geerlings, J. Lin and W. S. Chin, *Int. J. Hydrogen Energy*, 2010, **35,** 176-180.
29 A. C. Stowe, W. J. Shaw, J. C. Linehan, B. Schmid and T. Autrey, *Phys. Chem. Chem. Phys.*, 2007, **9,** 1831-1836.
30 H. W. Brinks and B. C. Hauback, *J. Alloys Compd.*, 2003, **354,** 143-147.